

## AN ELEMENT-BASED FINITE VOLUME FORMULATION FOR RESERVOIR SIMULATION

**Fernando Sandro Velasco Hurtado**

**Clovis Raimundo Maliska**

**Antônio Fábio Carvalho da Silva**

**Jonas Cordazzo**

fernando@sinmec.ufsc.br

maliska@sinmec.ufsc.br

afabio@sinmec.ufsc.br

jonas@sinmec.ufsc.br

SINMEC Lab, Department of Mechanical Engineering, Federal University of Santa Catarina, 88040-900, Florianopolis, BRAZIL

**Abstract.** *In this work is presented a numerical formulation for reservoir simulation in which the element-based finite volume method (EbFVM) is applied to the discretization of the differential equations that describe macroscopic multiphase flow in petroleum reservoirs. The spatial discretization is performed by means of quadrilateral unstructured grids, which are adequate for representing two-dimensional domains of any complexity in an accurate and efficient manner. For dealing with the inherent geometric complexity, all operations related to the discretization are performed at element level in a way that resembles the finite element method. However, the EbFVM approach preserves also the essence of conventional finite volume method, that is, the construction of approximate equations that guarantee the conservation of physical quantities at discrete level. One of the most promising aspects of the numerical formulation presented herein is the possibility of eliminating the so-called grid orientation effect, which is an abnormal dependence of numerical solutions on the grid geometry, which is present in all customary numerical methodologies used in reservoir simulation. As showed in several examples, an interpolation scheme consistent with the multidimensional character of the flow is the key factor for eliminating grid orientation effect. Other application examples are presented also for evaluating other aspects of the proposed numerical formulation.*

**Keywords:** *Reservoir Simulation, Unstructured Grids, EbFVM.*

## 1. INTRODUCTION

Nowadays one of the major challenges for reservoir simulation is the incorporation of the very detailed information coming from geological reservoir models into the numerical simulations. Thanks to the accelerated improvement in geosciences techniques, accurate reservoir static models including detailed description of all geological objects are currently available. Unfortunately, most of the discretization methods commonly used in reservoir simulation, mainly based on structured grids, are not capable to represent the detailed geometry of such geological objects or other complicated entities such as horizontal wells. As pointed out for several authors (Fung et al., 1992; Verma & Aziz, 1997; Heinemann & Heinemann, 2001) the key solution for that issue is the use of unstructured grids for representing the reservoir geometry into the dynamic models.

Although the use of unstructured grids for fluid flow simulation in complex geometries is currently a customary practice in several engineering areas, still little effort has been made in the reservoir simulation area for taking advantage of all the potential of unstructured grids. A large amount of research has been made with Voronoi or PEBI grids (Heinemann & Brand, 1989; Palagi & Aziz, 1992), which are locally orthogonal unstructured grids. This geometric feature allows using undemanding numerical procedures, similar to those habitually employed with structured grids, at least for isotropic porous media. A generalization of Voronoi grids was proposed in order to overcome that restriction, imposing special constraints on the grid generation. Unfortunately, those constraints are difficult to satisfy for complex geometries and highly anisotropic and heterogeneous media.

The so-called control-volume finite element method (CVFEM), developed at first for solving the Navier-Stokes equations, is the best alternative for discretizing conservation equations arising in reservoir dynamical models. Unstructured element grids can be used to represent arbitrarily complex geometries without regarding on the heterogeneity or anisotropy of the medium. In reservoir simulation, such discretization method has been applied mainly with triangular grids (Forsyth, 1990; Gottardi & Dall'olio, 1992; Fung et al., 1992; Fung et al., 1994). Numerical approximations used with this type of grids permit arranging the discretized equations in a form similar to those arising from conventional finite difference methods. Although this characteristic is advantageous at first, because it facilitates the implementation of CVFEM formulations into existing reservoir simulators, several drawbacks arises from that practice. As discussed by Cordazzo et al. (2004a), some of the approximations considered in those formulations are questionable for multiphase flow and lead to erroneous interpretations of the coefficients on the discretization equations. As a result, numerical simulations can exhibit non-physical behavior in several situations, as showed in Cordazzo et al. (2004b).

Differently from the classical finite element approach, local and global mass conservation can be directly enforced in the CVFEM approach, because of the construction of the discretized equations following the philosophy of the finite volume method. That is, discretized equations represent physical balances over control volumes, which are formed by element contributions. Because of this, we prefer to designate methods of that nature as element-based finite volume methods (EbFVM), since elements are used only as supporting geometric entities and no mathematical foundation of the finite element method is actually considered for discretizing the differential equations (Maliska, 2004).

In this work is described an EbFVM formulation for reservoir simulation considering quadrilateral unstructured grids. Differently from existent formulations on triangular grids, any attempt of adapting discretized equations to conventional forms is discarded. Thus, for example, the concept of transmissibility is completely abandoned. Most of the ideas applied for developing the formulation presented herein were originally proposed for the solution of the Navier-Stokes equations by Raw (1985). Maybe the most important feature of our formulation is the use of multidimensional interpolation schemes for approximating more accurately the advection-type terms in differential equations. As will be shown in this work, this is the key issue for eliminating the so-called grid orientation effect, which is a still unresolved problem in reservoir simulation.

## 2. ELEMENT-BASED FINITE VOLUME FUNDAMENTALS

For the application of the EbFVM to the discretization of differential equations describing a flow, the solution domain must be broken up into much smaller sub-domains, called *elements*, which in this work are quadrilaterals. These entities are used for defining the discretized geometry of the domain as well as for defining the spatial variation of medium physical properties. The unknowns of the problem are calculated at points called *nodes*, located at every element corner. Around every node is built a *control volume*, formed by portions of the elements sharing a common node. Every control volume is delimited by a certain number of *faces*, obtained joining the center of every neighboring element with the midpoint of its two sides sharing the node around which the control volume is built. As the surface integrals over the control-volume faces are usually approximated by the midpoint rule (Raw, 1985), the face center points are commonly known as *integration points*. All these geometrical entities are depicted in Fig. 1.

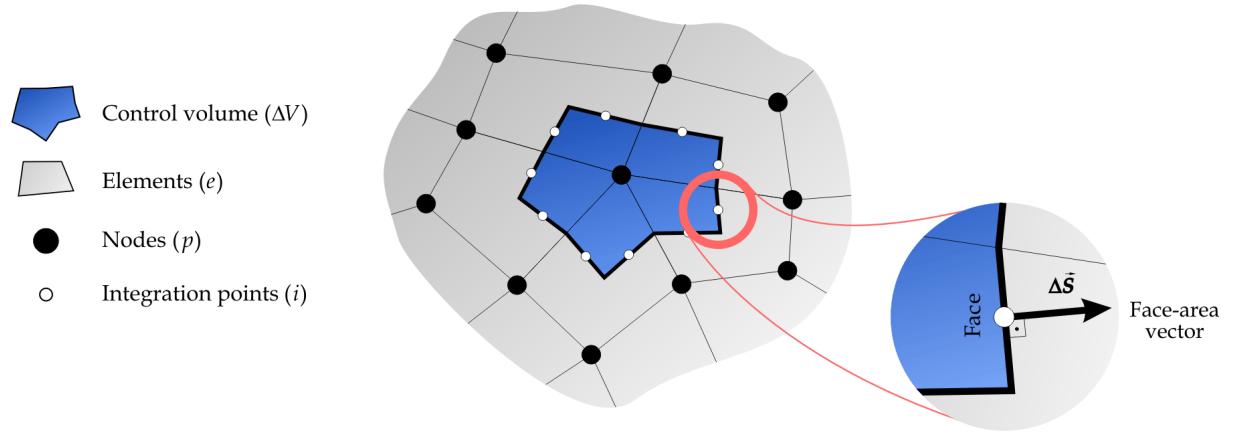


Figure 1 - Main geometrical entities on the element-based finite volume method.

As in any finite volume methodology, the conservation of physical quantities over every control volume is the essential premise of the EbFVM. However, since the shape of control volumes constructed following the described procedure can become extremely complex, a special strategy is required for dealing with the increased geometrical complexity. The strategy employed in the EbFVM, borrowed from the finite element technique, is the definition of a local coordinate system  $\xi, \eta$  inside every element. Therefore, all needed calculations can be easily made based upon the geometry of isolated transformed elements, and then conservation equations of every control volume can be simply assembled using the contributions coming from all neighboring elements. For quadrilateral elements, the coordinate transformation can be conveniently expressed employing the bilinear shape functions (Maliska, 2004)

$$\begin{cases} N_1(\xi, \eta) = \frac{1}{4}(1 + \xi)(1 + \eta); & N_2(\xi, \eta) = \frac{1}{4}(1 - \xi)(1 + \eta); \\ N_3(\xi, \eta) = \frac{1}{4}(1 + \xi)(1 - \eta); & N_4(\xi, \eta) = \frac{1}{4}(1 - \xi)(1 - \eta) \end{cases} \quad (1)$$

The local coordinates  $\xi, \eta$  can be related to the ones on a global coordinate system by means of the transformation equations

$$\begin{cases} x(\xi, \eta) = \sum_{j=1}^4 N_j(\xi, \eta) x_j \\ y(\xi, \eta) = \sum_{j=1}^4 N_j(\xi, \eta) y_j \end{cases} \quad (2)$$

Here,  $x_j$  and  $y_j$  are the global coordinates at the  $j$ -th node of a given element, when a local node numbering, like the conventional one shown in Fig. 2(a) is employed. No matter how distorted one element might be in terms of global coordinates, its representation in terms of local coordinates is always a regular square element, as shown in Fig. 2(b).

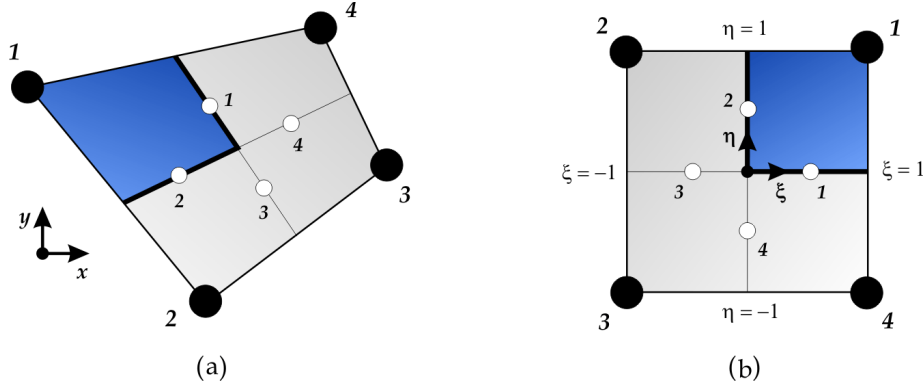


Figure 2 - Isolated element in global and local coordinate system.

For evaluating fluxes at the faces inside an element usually one need to approximate the gradient of a continuous variable at integration points. Assuming a bilinear variation for a generic variable  $\Theta$  inside an element, similar to that considered for global coordinates, the following approximation for its gradient can be obtained (Hurtado, 2005)

$$[\nabla\Theta] \approx [J]^{-1}[D][\Theta]_e \quad (3)$$

Here,  $[\Theta]_e$  is a column vector containing the values of the variable  $\Theta$  at the four nodes in an element. Moreover,  $[D]$  is an auxiliary matrix containing all first-order partial derivatives of the shape functions, ordered in the following way

$$[D] = \begin{bmatrix} \partial_{\xi} N_1 & \partial_{\xi} N_2 & \partial_{\xi} N_3 & \partial_{\xi} N_4 \\ \partial_{\eta} N_1 & \partial_{\eta} N_2 & \partial_{\eta} N_3 & \partial_{\eta} N_4 \end{bmatrix} \quad (4)$$

In addition,  $[J]$  is the Jacobian matrix of the coordinate transformation. This matrix can be easily obtained with the derivative matrix  $[D]$  by means of

$$[J] = [D][\Omega]_e \quad (5)$$

where  $[\Omega]_e$  is a  $4 \times 2$  matrix containing the global coordinates  $x_j$  and  $y_j$  of the four nodes located at the vertices of the given element, ordered according the local node numbering showed in Fig. 2.

Similar relationships can be obtained for all geometric parameters needed for the discretization process, in terms of the local coordinate system. Further details can be found elsewhere (Hurtado, 2005; Raw, 1985).

### 3. MATHEMATICAL FLOW MODEL

For the sake of simplicity, the numerical formulation presented in this work will be described considering a two-phase incompressible and immiscible flow model. The discretization process for a more complex flow model certainly will share all geometry-related issues that will be discussed for two-phase incompressible model. Though, a more general formulation including fluid compressibility, capillary pressure, and gravity is described in Hurtado (2005) and Hurtado et al. (2004).

For incompressible fluids, the mass-conservation differential equations have the form

$$\phi \partial_t s_\alpha + \vec{\nabla} \cdot \vec{v}_\alpha = 0 ; \quad \alpha = I, D \quad (6)$$

Here the two fluid phases are denoted as *invading phase* (*I*) and *displaced phase* (*D*). Moreover,  $s_\alpha$  and  $\vec{v}_\alpha$  are the saturation and the mean velocity vector of the given phase, respectively;  $\phi$  is the porosity of the medium, which is assumed independent of time. The mean velocity of each phase is related to the pressure gradient by means of the extension of Darcy's law for multiphase flow. The mathematical expression of this law is given by

$$\vec{v}_\alpha = -\lambda_\alpha \vec{\mathbf{K}} \cdot \vec{\nabla} P ; \quad \alpha = I, D \quad (7)$$

In this expression,  $P$  is the pressure,  $\vec{\mathbf{K}}$  is the tensor of absolute permeability of the medium, and  $\lambda_\alpha$  is the phase mobility, which is defined as

$$\lambda_\alpha = \frac{k_{r\alpha}}{\mu_\alpha} ; \quad \alpha = I, D \quad (8)$$

Here  $k_{r\alpha}$  and  $\mu_\alpha$  are the phase relative permeability and the phase viscosity, respectively. Typically, relative permeabilities are considered function of the phase saturations. In the model considered herein, both absolute permeability and porosity can be function of space coordinates.

The volumetric constraint equation closes the system of equations describing the flow. For two-phase flow this equation is

$$s_I + s_D = 1 \quad (9)$$

Although Eq. (6) together with Eqs. (7) and (9) describe adequately immiscible two-phase flow, an alternative pair of differential equations is more convenient for characterizing mathematical properties (Peaceman, 1977) and constructing a numerical formulation. These equations are the *pressure equation*

$$\vec{\nabla} \cdot (\lambda_T \vec{\mathbf{K}} \cdot \vec{\nabla} P) = 0 \quad (10)$$

and the *saturation equation* for the invading phase, arranged in the so-called Buckley-Leverett form (Peaceman, 1977)

$$\phi \partial_t s_I + \vec{\nabla} \cdot (F_I \vec{v}_T) = 0 \quad (11)$$

where  $\lambda_T = \lambda_I + \lambda_D$  is the total mobility, and  $\vec{v}_T = \vec{v}_I + \vec{v}_D$  is the total velocity. Furthermore,  $F_I = \lambda_I / \lambda_T$  is known as fractional flux function, which depends only on the saturation  $s_I$ . The total velocity has the role of coupling variable between pressure and saturation equations, by means of

$$\vec{v}_T = -\lambda_T \vec{\mathbf{K}} \cdot \vec{\nabla} P \quad (12)$$

It is easy to realize that pressure Eq. (10) is an elliptic equation, whereas saturation Eq. (11) is a non-linear hyperbolic equation. As will be shown further, the comprehension of the nature of the differential equations is very important when selecting interpolation schemes for the numerical approximation of those equations.

#### 4. NUMERICAL FORMULATION

A sequential solution approach will be considered for constructing the numerical formulation for solving the two-phase flow inside a reservoir. Therefore, the time evolution of dependent variables, namely pressure and saturation, will be obtained solving separately discrete analogs of Eqs. (10) and (11). In this section the EbFVM is applied for discretizing those equations.

The integration of pressure equation over a generic control volume like the one depicted in Fig. 1, leads to

$$\int_{\Delta V} \vec{\nabla} \cdot (\lambda_T \vec{\mathbf{K}} \cdot \vec{\nabla} P) dV = 0 \quad (13)$$

The application of the divergence theorem permits to transform the volume integral into a surface integral. Furthermore, the resulting surface integral can be broken up into several integrals defined over control volume faces, that is

$$\int_{\cup \Delta S_i} (\lambda_T \vec{\mathbf{K}} \cdot \vec{\nabla} P) \cdot d\vec{\mathbf{S}} = \sum_i \int_{\Delta S_i} (\lambda_T \vec{\mathbf{K}} \cdot \vec{\nabla} P) \cdot d\vec{\mathbf{S}} = 0 \quad (14)$$

Approximating these integrals by means of the midpoint rule (Raw, 1985) permits to derive the following discrete analog of Eq. (10) at time level  $n$

$$\sum_e \left\{ \sum_i (\lambda_T)_i^n \left[ \vec{\mathbf{K}} \cdot (\vec{\nabla} P)_i^n \right] \cdot \Delta \vec{\mathbf{S}}_i \right\} = 0 \quad (15)$$

Here the variables are related to integration points  $i$ , which are located at face centers;  $\Delta \vec{\mathbf{S}}_i$  denotes the area vector associated to a face, pointing outside of the control volume, as depicted in Fig. 1. The sum in Eq. (15) must be performed over all elements  $e$  surrounding a control volume. Since the pressure equation is elliptic, a bilinear approximation is suitable for the pressure variation inside an element (Raw, 1985), so Eq. (3) can be used for approximating pressure gradient. It can be shown (Hurtado, 2005) that this permits writing

$$\left\{ (\lambda_T)_i^n \left[ \vec{\mathbf{K}} \cdot (\vec{\nabla} P)_i^n \right] \cdot \Delta \vec{\mathbf{S}}_i \right\} \approx (\lambda_T)_i^n [b]_i^T [P]_e^n \quad (16)$$

for a given integration point  $i$  inside an element  $e$ . Here  $[P]_e^n$  is a column vector whose components are the four nodal values of pressure in the element, and  $[b]_i^T$  is a row vector defined as

$$[b]_i^T \equiv [\Delta S]_i^T [K]_e [J]_i^{-1} [D]_i \quad (17)$$

where  $[\Delta S]_i$  is the face area column vector,  $[K]_e$  is the matrix form of permeability tensor for the element, and  $[J]_i$  and  $[D]_i$  are the Jacobian matrix and the derivatives matrix defined in section 2, both evaluated at the given integration point.

The vector  $[b]_i^T$  has a distant connection with the transmissibility concept, used in traditional numerical formulations for reservoir simulation (Cordazzo et al., 2002), because it depends on geometric parameters and medium properties only. The situation is different here, however, because flow rate across a face is not anymore proportional to a difference between two nodal values of pressure as usually happens when dealing with orthogonal grids. As showed by Eq. (16), in the EbFVM approach, the flow rate across a face depends on the pressure values at the four nodes of an element. It is remarkable also that a full permeability tensor, possibly varying from element to element, can be included into the formulation without increasing its complexity at all.

For assembling the complete discrete equation (15) for all control volumes, it will be considered an assembling procedure similar to that used in the finite element method. In order to make this possible, the contributions of an element to the conservation equations of the four adjoining control volumes must be arranged into the following matrix form

$$\left\{ \sum_i (\lambda_T)_i^n \left[ \vec{\mathbf{K}} \cdot (\vec{\nabla} P)_i^n \right] \cdot \Delta \vec{\mathbf{S}}_i \right\} \approx \begin{bmatrix} (\lambda_T)_1^n [b]_1^T - (\lambda_T)_2^n [b]_2^T \\ (\lambda_T)_2^n [b]_2^T - (\lambda_T)_3^n [b]_3^T \\ (\lambda_T)_3^n [b]_3^T - (\lambda_T)_4^n [b]_4^T \\ (\lambda_T)_4^n [b]_4^T - (\lambda_T)_1^n [b]_1^T \end{bmatrix} \begin{bmatrix} P_1 \\ P_2 \\ P_3 \\ P_4 \end{bmatrix} \equiv [A]_e [P]_e^n \quad (18)$$

The matrix  $[A]_e$  is called herein as element matrix. Each row of this matrix is related to one of the four adjoining control volumes and includes two contributions because always two faces on a control-volume border lay inside an element, as shown in Fig. 2. The subscripts in Eq. (18) are related to the integration point numbering depicted also in Fig. 2. Moreover, Eq. (18) assumes that face-area vectors inside an element have fixed orientation, so a given face-area vector is positive in relation to one of the adjoining control volumes and negative in relation to the other. Due to that fact the two contributions in a row of an element matrix have opposite signs.

The global coefficient matrix for the pressure equation system will be obtained after summing all element matrix contributions for all control volumes, according to the assembling procedure depicted schematically in Fig. 3. Since no other terms exist in the pressure differential equation, the vector of independent terms for the pressure equation system will include only boundary condition parameters, or more specifically, well parameters. So we will have completely defined

$$[A][P]^n = [B] \tag{19}$$

The solution of this linear system will provide an approximation of the pressure field for a given phase-distribution in the solution domain at a time level  $n$ .

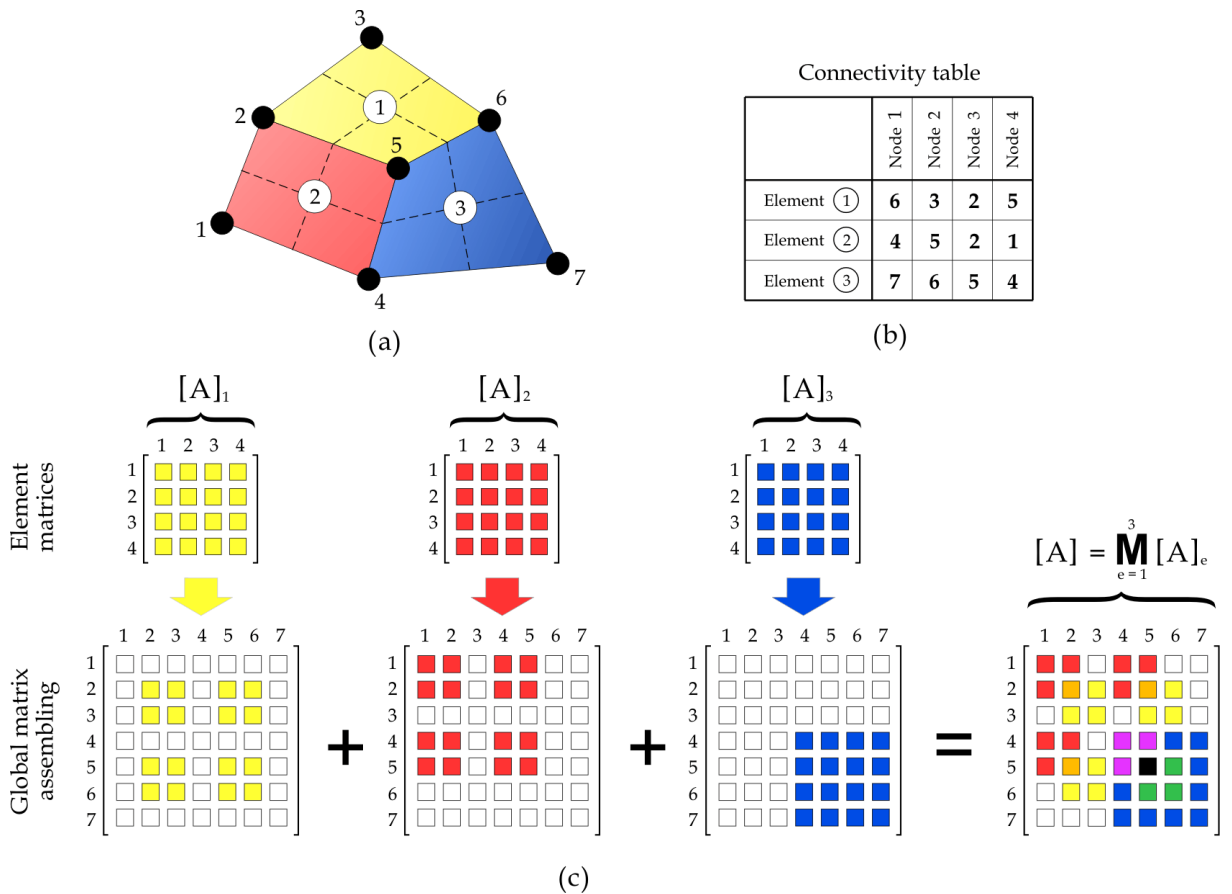


Figure 3 - Schematic representation of the matrix assembling procedure for a three-element grid.

In order to complete the solution process, after computing the pressure at time level  $n$ , the saturation should be advanced to the next time level. A discrete equivalent of differential Eq. (11) must be obtained for performing this step. The integration of that equation over a control volume gives

$$\int_{\Delta V} \partial_t(s_l) \phi dV + \sum_i \int_{\Delta S_i} F_l \bar{\mathbf{v}}_T \cdot \mathbf{d}\bar{\mathbf{S}} = 0 \tag{20}$$

Approximating the integrals again by means of the mid-point rule and the time derivative by means of a backward finite difference scheme, the following discrete equation is obtained

$$\left[ \frac{(s_l)_p^{n+1} - (s_l)_p^n}{\Delta t^n} \right] \phi_p \Delta V_p + \sum_i (F_l)_i^n (q_T)_i^n = 0 \quad (21)$$

where  $(q_T)_i^n$  is the total volumetric flow rate across a control volume face, given by

$$(q_T)_i^n = (\vec{v}_T)_i^n \cdot \Delta \vec{S}_i \approx -(\lambda_T)_i^n [b]_i [P]_e^n \quad (22)$$

This volumetric flow rate can be easily computed after solving the pressure linear system. From Eq. (21), it follows that

$$(s_l)_p^{n+1} = (s_l)_p^n - \frac{\Delta t^n}{\phi_p \Delta V_p} \sum_i (F_l)_i^n (q_T)_i^n \quad (23)$$

This explicit discrete equation can be used for advancing saturation to time level  $n+1$ . This step resembles the traditional IMPES algorithm, though a slightly different approach was used in this work. Since Eq. (23) has a severe time-step stability restriction, a special strategy was considered for accelerating the performance of the solution process. Since the total velocity field frequently evolves much slowly than saturation field, that velocity field can be kept frozen during a certain period of time in which only saturation is advanced, using a stable time-step. Following that practice, it is no more required to solve pressure linear system every time that saturation is updated. Consequently, significant computation-time savings can be obtained without appreciable declining in quality. This solution strategy is discussed more deeply in Hurtado (2005).

## 5. SPATIAL INTERPOLATION SCHEME

An important issue arises concerning the interpolation scheme for computing  $(F_l)_i^n$  at integration points in Eq. (23). Since saturation differential equation is hyperbolic, linear-type interpolations are not suitable because it produces unrealistic solutions with spurious spatial oscillations and unbounded values (Peaceman, 1977). In order to avoid this, upwind-type interpolation schemes are commonly used in reservoir simulation. However, the customary approach is to use one-dimensional upwind schemes along grid lines. This causes an undesirable and frequently strong dependence of the numerical solutions on the computational grid, the so-called *grid orientation effect* (Brand et al., 1991).

Taking advantage of the increased geometric flexibility provided by the EbFVM discretization approach, we used an interpolation scheme that takes into account the multidimensional nature of the flow. This is the point that distinguishes our formulation from customary numerical formulations used in reservoir simulation. The original form of the interpolation scheme considered herein was proposed for approximating the advection terms in the Navier-Stokes equations (Schneider & Raw, 1986). It has two fundamental features: the absolute preservation of the positivity of the discretized equation coefficients and the consideration of the flow local direction.

In order to define the interpolation scheme, which will be designated herein as flow-weighted upwind scheme (FWUS), it is needed to consider a local flow ratio. For a given integration point, that parameter is defined as the ratio of the total flow rate across the upwind face and total flow rate across the face where the integration point is located. For instance, the flow ratio at integration point 1, for a positive flow orientation (pointing to local node 4) will be

$$\omega_1 = \frac{(q_T)_2}{(q_T)_1} \quad (24)$$

Figure 4 shows three cases considered in the interpolation scheme originally proposed by Schneider & Raw (1986). They correspond to integration point 1 and are determined by



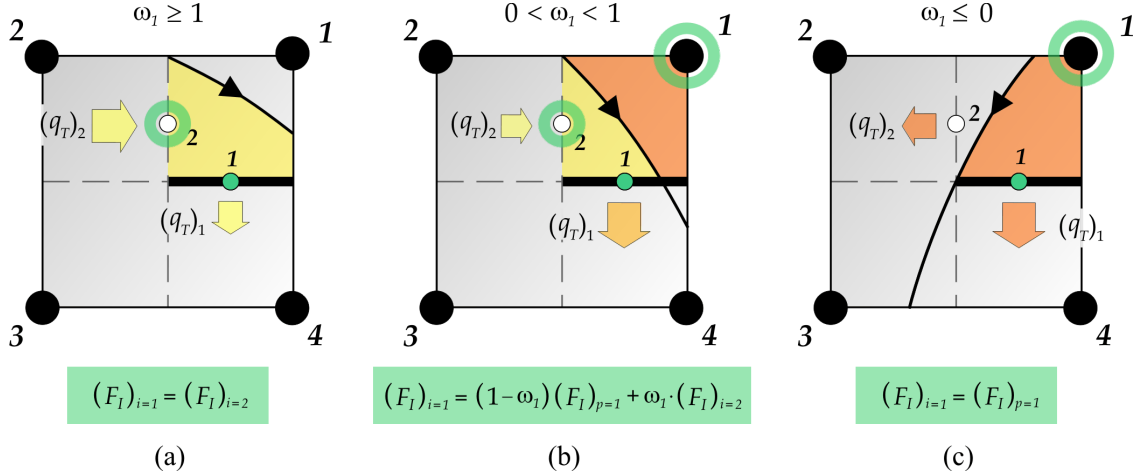


Figure 4 – Three cases considered in the flow-weighted interpolation scheme.

the flow ratio value. For the interval  $0 < \omega_1 < 1$ ,  $(F_I)_{i=1}$  is considered a linear combination of  $(F_I)_{i=2}$  and  $(F_I)_{p=1}$  because a portion of the flow passing through the face 1 comes from face 2, transporting by advection integration point value  $(F_I)_{i=2}$ , and another portion comes from inside the control volume, thus carrying nodal value  $(F_I)_{p=1}$ . This is schematically depicted in Fig. 4(b). In that case, the flow ratio  $\omega_1$  is taken as interpolation factor because it determines the proportion of the fluid that passes through face 1 and comes from face 2.

Two limiting cases can be considered in the interpolation scheme. One of them, depicted in Fig. 4(a), arises when  $\omega_1 \geq 1$ . In this case all the fluid flowing across face 1 comes from face 2, consequently it is stated that  $(F_I)_{i=1} = (F_I)_{i=2}$ . The opposite case occurs when  $\omega_1 \leq 0$ , as can be seen in Fig. 4(c). Now all flow comes from inside the control volume to which face 1 belongs, transporting by advection the nodal value associated to it, so it is considered  $(F_I)_{i=1} = (F_I)_{p=1}$  in this case. Similar reasoning is applicable to all integration points inside an element. In the end, all described cases for integration point 1 can be summarized in the expression

$$(F_I)_{i=1} = (1 - \Lambda_1)(F_I)_{p=1} + \Lambda_1 \cdot (F_I)_{i=2} \quad (25)$$

where the interpolation factor is given by

$$\Lambda_1 = \max[\min(\omega_1, 1), 0] \quad (26)$$

It is possible to show that the upwind interpolation scheme defined by Eqs. (25) and (26) generates discrete advection operators with always positive coefficients (Schneider & Raw, 1986, Hurtado, 2005). This assures that no spurious spatial oscillations or unbounded values arise in the saturation field, an essential requirement for reservoir simulation. The local direction of total flow is accounted for introducing the flow ratio into the interpolation scheme. Therefore, the adverse grid influence exhibited by conventional upwind schemes is reduced significantly, even in the more unfavorable cases. For reducing grid orientation effect, we achieved even better results substituting Eq. (26) by smooth functions  $\Lambda_i = \Lambda_i(\omega_i)$  which are tangent to  $\Lambda_i = \omega_i$  at  $\omega_i = 0$  and that reach asymptotically the limiting value  $\Lambda_i = 1$  for  $\omega_i \rightarrow \infty$ . In the next section several examples using those interpolation functions will be presented, showing practically no grid orientation effect.

## 6. APPLICATION EXAMPLES

Two application examples of the proposed formulation are presented in this section. The first problem is the simulation of oil secondary recovery in a faulted reservoir. The quadrilateral unstructured grid used for discretizing a fictitious reservoir is shown in Fig. 5. Local refinement is

considered in regions around wells (one injection and two production wells) since usually more accurate solutions are required in those regions. A geological fault is modeled as an internal impermeable boundary, so the grid was enforced to adapt to the geometry of this boundary. Although our formulation is able to deal with heterogeneous and anisotropic media, in this example was considered a uniform and isotropic medium. Figure 6 shows the time evolution of water saturation in the reservoir, predicted using the present numerical formulation.

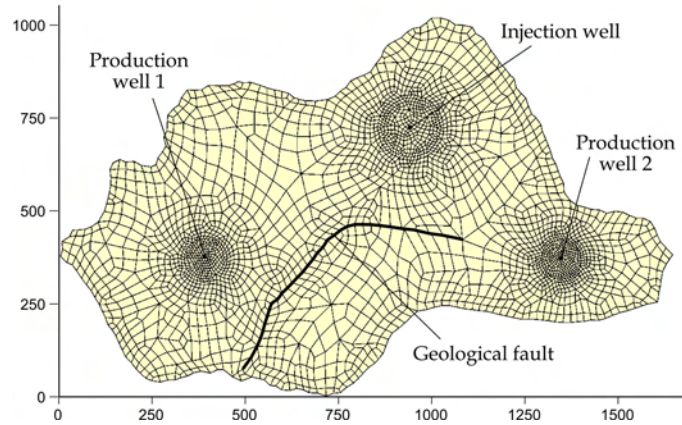


Figure 5 – Unstructured grid with local refinement for a faulted reservoir.

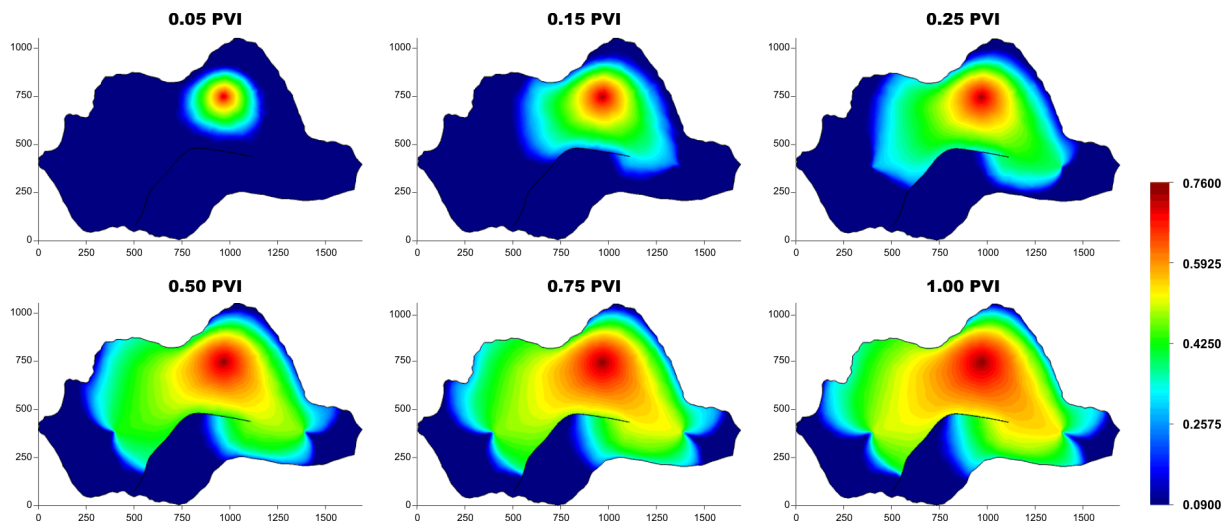


Figure 6 – Predicted time evolution of water saturation in the faulted reservoir.

As second example is considered the five-spot problem, a well-known test for evaluating the grid orientation effect. It consists in the simulation of a water-oil displacement in a periodic arrangement of injection and production wells, as illustrated in Fig. 7. Due to symmetry, two Cartesian grids in simple square domains can be used to solve the flow, the so-called diagonal and parallel grids (see Fig. 7). Ideally, the numerical solution in any grid should be the same, or at least nearly the same, but this is not the case when conventional formulations are used in adverse cases (Brandt, 1991). The most adverse situations arise when the mobility of the water (invading phase) is greater than the mobility of the oil (displaced phase) and a strong discontinuity develops in the saturation field. In order to enforce a piston-type displacement, according to Yanosik & McCracken (1979) the fractional-flux function was defined as

$$F_l = \hat{s}_l^2 \tag{27}$$

where  $\hat{s}_i$  is a normalized saturation. Moreover, a water/oil mobility ratio value of 10 was considered for obtaining the numerical solutions presented subsequently.

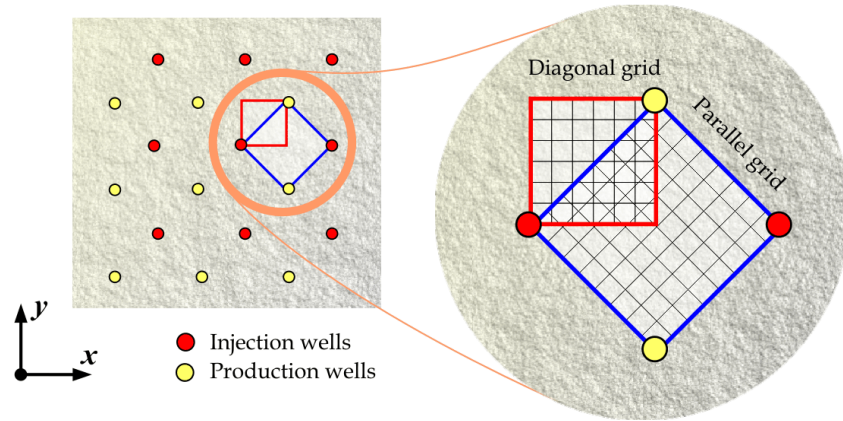


Figure 7 – Schematic diagram of five-spot well arrangement.

Figure 8 presents a comparison of predicted saturation isolines, obtained in a 400-element diagonal grid and in a 784-element parallel grid employing three upwind interpolation schemes. The solutions in Fig. 8(a) were obtained with the one-dimensional upwind scheme along grid lines, ordinarily used in conventional numerical formulations. As can be observed, a significant discrepancy exists in that case between diagonal-grid and parallel-grid solutions. Better agreement

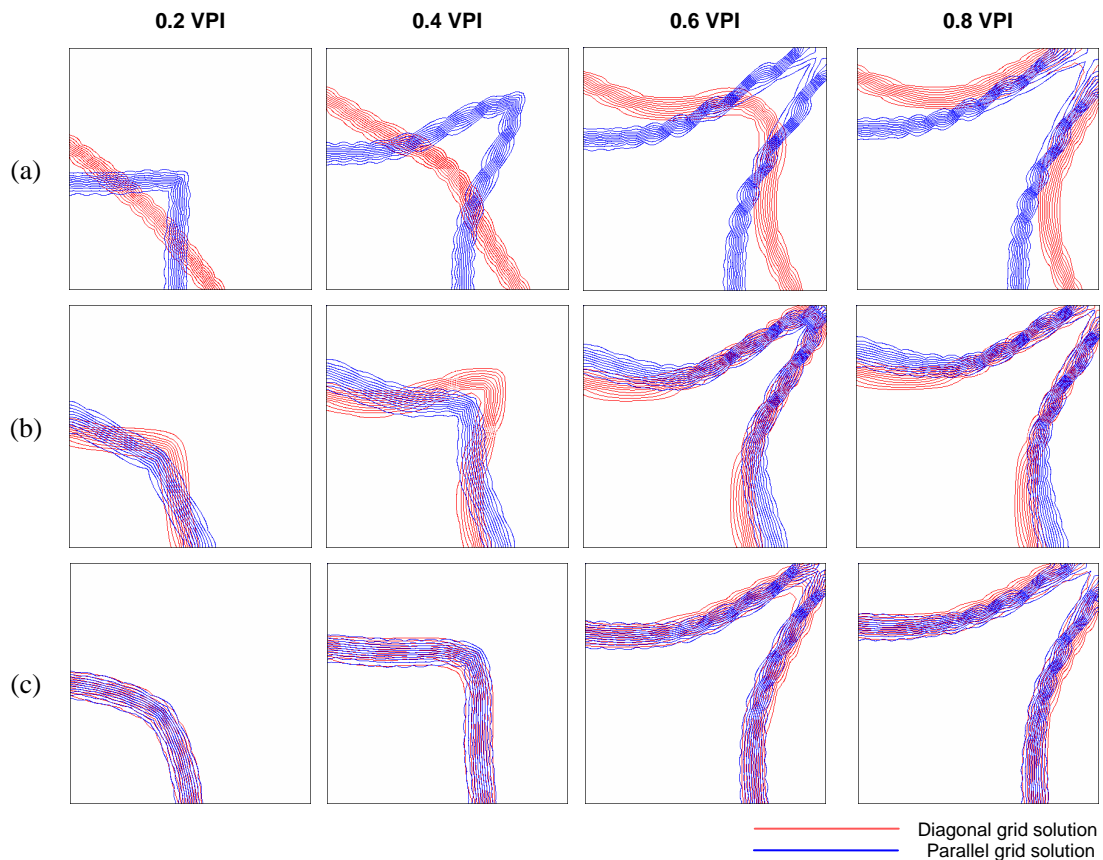


Figure 8 – Comparison of diagonal-grid and parallel-grid solutions for a piston-type displacement in a quarter of a five-spot configuration, using (a) conventional upwind interpolation; (b) Schneider & Raw's FWUS; and (c) FWUS with  $\Lambda_i$  given by Eq. (28).

is obtained using the flow-weighted upwind scheme of Schneider & Raw, defined by Eqs. (25) and (26). The solutions with that scheme are showed in Fig. 8(b). However, even better agreement is achieved employing an interpolation factor defined by the smooth function

$$\Lambda_i = \max [\omega_i / (\omega_i + 1), 0] \quad (28)$$

Solutions with that scheme are compared in Fig. 8(c). As can be clearly seen, almost no grid orientation effect is noticeable in those solutions. Relating the interpolation scheme to the local flow direction through the flow rate ratio has the effect of removing practically all anomalous influence of the grid on the numerical solutions. In order to demonstrate the behavior of the interpolation scheme with unstructured grids, the previous problem was solved using the two grids that are showed in Fig. 9, a 440-element ‘diagonal’ grid and a 790-element ‘parallel’ grid. The solutions obtained in those grids are compared in Fig. 10. Again no significant differences among solutions are perceptible. Further evaluation of the performance of the flow-weighted interpolation scheme in reservoir simulation can be found in Hurtado (2005).

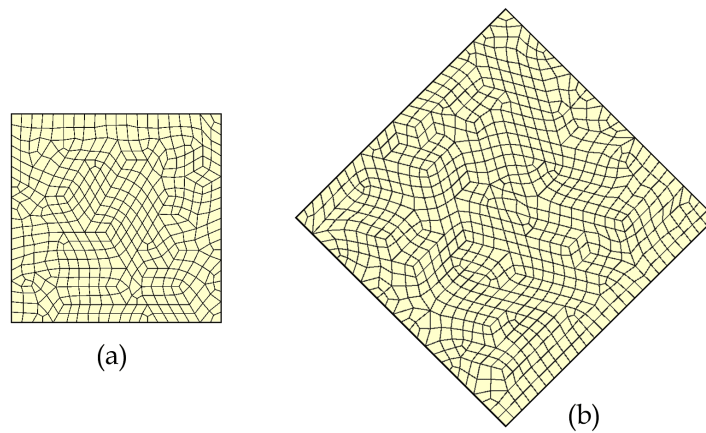


Figure 9 – Unstructured ‘diagonal’ and ‘parallel’ grids.

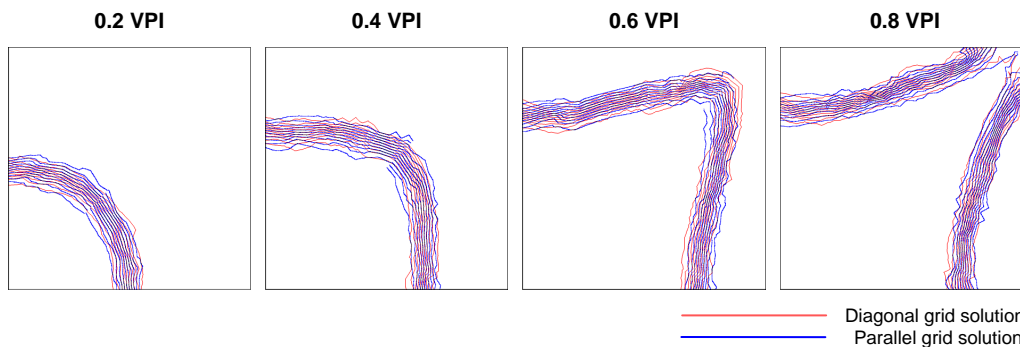


Figure 10 – Comparison of solutions in a quarter of a five-spot configuration, obtained in unstructured ‘diagonal’ and ‘parallel’ grids.

## 7. CONCLUDING REMARKS

An element-based finite volume formulation using quadrilateral unstructured grids has been presented in this paper. Although a two-phase incompressible flow model was considered for describing the discretization of differential equations, a more general formulation, e.g. one based on the black-oil model, can be straightforwardly constructed since all geometry-related issues will be essentially the same considered in this work.

As seen in two application examples, our formulation has two major advantages over the common numerical methodologies used in reservoir simulation. First, it has increased geometrical flexibility for accurately represent complex reservoirs with local grid refinement in regions of special interest. And second, truly multidimensional upwind schemes can be easily implemented in the element-based framework. As showed in the five-spot example, the flow-weighted upwind scheme used in this work resulted in numerical solutions with virtually no grid orientation effect. Certainly, these advantages should encourage further developments in reservoir simulation applying the element-based finite volume methodology.

## 8. ACKNOWLEDGEMENTS

This work was supported by Agência Nacional do Petróleo (ANP), through PRH 09 - Programa de Formação de Recursos Humanos em Petróleo e Gás.

## 9. REFERENCES

- Brand, C. W., Heinemann, J. E., Aziz, K., 1991. The grid orientation effect in reservoir simulation. Paper SPE 19353, *11<sup>th</sup> Symposium on Reservoir Simulation*, Anaheim, USA.
- Cordazzo, J., Maliska, C. R. & Silva, A. F. C., 2002. Interblock transmissibility calculation analysis for petroleum reservoir simulation. *Proceedings of the 2<sup>nd</sup> Meeting on Reservoir Simulation*, November 5-6, Buenos Aires, Argentina.
- Cordazzo, J., Maliska, C. R., Silva, A. F. C. & Hurtado, F. S. V., 2004a. The negative transmissibility issue when using CVFEM in petroleum reservoir simulation - 1. Theory. *Proceedings of the 10<sup>th</sup> Brazilian Congress of Thermal Sciences and Engineering*, November 30-December 3, Rio de Janeiro, Brazil.
- Cordazzo, J., Maliska, C. R., Silva, A. F. C. & Hurtado, F. S. V., 2004b. The negative transmissibility issue when using CVFEM in petroleum reservoir simulation - 2. Results. *Proceedings of the 10<sup>th</sup> Brazilian Congress of Thermal Sciences and Engineering*, November 30-December 3, Rio de Janeiro, Brazil.
- Forsyth, P. A., 1990. A control-volume finite element method for local mesh refinement in thermal reservoir simulation. *SPE Reservoir Engineering*, Vol. November 1990, pp. 561-566.
- Fung, L. S., Buchanan L. & Sharma, R., 1994. Hybrid-CVFE method for flexible-grid reservoir simulation. *SPE Reservoir Engineering*, Vol. August 1994, pp. 188-194.
- Fung, L. S., Hiebert, A. D. & Nghiem L., 1992. Reservoir simulation with a control-volume finite-element method. *SPE Reservoir Engineering*, Vol. August 1992, pp. 349-357.
- Gottardi, G. & Dall'olio, D., 1992. A control-volume finite-element model for simulating oil-water reservoirs. *Journal of Petroleum Science and Engineering*, Vol. 8, pp. 29-41.
- Heinemann, G. F. & Heinemann, Z. E., 2001. Gridding concept for the third generation of reservoir simulators. *Sixth International Forum on Reservoir Simulation*, September, 3-7, Salzburg, Austria.
- Hurtado, F. S. V., 2005. *An element-based finite volume formulation for the simulation of two-phase immiscible flow in porous media*. M.Sc. Dissertation (in Portuguese), Mechanical Engineering Department, Federal University of Santa Catarina, Brazil.
- Hurtado, F. S. V., Maliska, C. R., Silva, A. F. C., Cordazzo, J., Ambrus, J. & Contessi, B. A., 2004. An element-based finite volume formulation for simulating two-phase immiscible displacements in core samples. *Proceedings of the 10<sup>th</sup> Brazilian Congress of Thermal Sciences and Engineering*, November 30-December 3, Rio de Janeiro, Brazil.
- Maliska, C. R., 2004. *Transferência de calor e mecânica dos fluidos computacional*, 2<sup>a</sup> edição revista e ampliada. Livros Técnicos e Científicos Editora S. A., Rio de Janeiro, Brasil.

- Peaceman, D. W., 1977. *Fundamentals of numerical reservoir simulation*, In Developments in Petroleum Science, Vol. 6, Elsevier Scientific Publishing Company.
- Raw, M. J., 1985. *A new control-volume-based finite element procedure for the numerical solution of the fluid flow and scalar transport equations*. Ph.D. Thesis, University of Waterloo, Canada.
- Schneider, G. E. & Raw, M. J., 1986. A skewed, positive influence coefficient upwinding procedure for control-volume-based finite-element convection-diffusion computation. *Numerical Heat Transfer*, Vol. 9, pp. 1-26.
- Verma, S. & Aziz, K., 1997. A control-volume scheme for flexible grids in reservoir simulation. SPE Paper 37999, presented at the *1997 Reservoir Simulation Symposium*, June 8-11, Dallas, USA.
- Yanosik, J. L. & McCracken, T. A., 1979. A nine-point, finite difference reservoir simulator for realistic prediction of adverse mobility ratio displacements. *SPE Journal*, Vol. August 1979, pp. 253-262.